www.czasopisma.pan.pl PAN www.journals.pan.pl

ARCHIVES of FOUNDRY ENGINEERING

ISSN (2299-2944)
Volume 18
Issue 2/2018

51 – 56

DOI: 10.24425/122502

10/2

Published quarterly as the organ of the Foundry Commission of the Polish Academy of Sciences

Modification Mechanism and Growth Process of $Al_3(Sc, Zr)$ Particles in As-cast Al-Si-Mg-Cu-Zr-Sc Alloy

Yukun Li, Xiaodong Du *, Junwei Fu, Ya Zhang, Zhen Zhang, Shiang Zhou, Yucheng Wu
Hefei University of Technology, School of Materials Science and Engineering,
Hefei 230009, China
* Corresponding author: E-mail address: hfutdxd@126.com

Received 03.02.2017; accepted in revised form 30.03.2018

Abstract

In this study, the modification mechanism and growth process of $Al_3(Sc, Zr)$ particles in as-cast Al-Si-Mg-Cu based alloy with addition of Sc and Zr were systematically investigated. It was found that 0.57 wt-%Sc addition caused a significant refinement in the average grain size of the investigated alloy, which brought about a remarkable transformation in as-cast microstructure, from thick dendritic shape to fine equiaxed structure. A large amount of primary $Al_3(Sc, Zr)$ particles with the dimension of around 5-6 μm were also observed within the equiaxed grain. Due to the identical orientation and similar crystal structure between primary $Al_3(Sc, Zr)$ particles and α-Al matrix, the primary particles always served as heterogeneous nucleus for the α-Al matrix. In addition, these cusped cubic primary $Al_3(Sc, Zr)$ particles showed triangle, star, rhomboid morphologies are generated from sectioning the particle in (111), (100) and (110) planes, respectively. Particularly, the typical eutectic structure which contained odd number-layer ($Al_3(Sc, Zr)$+α-Al+ ··· +$Al_3(Sc, Zr)$) was observed within the investigated particles.

Keywords: Solidification process, Metallography, $Al_3(Sc, Zr)$, Three-dimensional morphology, Eutectic growth

1. Introduction

Grain refinement is a crucial technique to refine the microstructure and enhance mechanical properties of casting Al alloys. The fine equiaxed structure is desirable in most castings which generally bring a lot of benefits. For instance, good mechanical performance and improved processing performance [1-5]. For several decades now, the microstructure refinement for casting Al alloy have been widely investigated in research institution for developing effective modifier. Considering actual industrial application environment, the modification of Al alloy are usually achieved by adding conventional master alloy refiners (e.g. Al-Ti/Al-Ti-B) into Al alloy [6]. Considerable researches have been done on the modification mechanism of these refiners. These theoretical researches focused on (a) heterogeneous nucleation, (b) growth restriction factor (Q) caused by constitutional undercooling [7-8]. These two factors are believed to play important roles in grain refinement, which result in the formation of small uniform equiaxed-grains. Nevertheless, there are still some drawbacks associated with the Al-Ti/Al-Ti-B refiners, such as their tendency to fade [9].

Another effective method to refine as-cast microstructure is microalloying with transition elements Er, Zr and Sc [10-13]. In previous studies, the influence of Sc addition on microstructural evolution and mechanical properties of Al alloys had been recognized. It had been declared that Sc could serve as more effective modifier than conventional master alloy refiners, which

does not suffer from fading and producing much finer as-cast microstructures [9, 14-17]. Zr is always added into Al alloy to replace a portion of Sc, due to its high price. Particularly, the growth restriction by Sc and Zr addition was small [18-21]. Therefore, heterogeneous nucleation act as the key factor of grain refinement.

However, up to now, few investigations have been reported on the modification mechanism in as-cast Al-Si-Mg-Cu-Sc-Zr alloy. The fundamental grain refinement mechanism of Sc and Zr addition to Al alloy is also not clear. Thus, the major objective of the present research is to investigate the modification mechanism of Al-Si-Mg-Cu-Sc-Zr alloy. In addition, the nucleation and growth modes of primary particle are also being detailed discussed.

2. Experimental details

The investigated Al-3Si-0.45Mg-0.45Cu-0.2Zr and Al-3Si-0.45Mg-0.45Cu-0.2Zr-0.6Sc alloys (wt-%, used throughout the paper unless noted otherwise) were prepared adopt the following casting process. The commercial raw alloys (purity Al (99.99), Al-21.54Si, Al-50.38Mg, Al-39.97Cu, Al-3.9Zr and Al-2.02Sc) were melted and mixed in a graphite crucible employing an electric resistance furnace. Degassing was performed to reduce dissolved hydrogen. The process carried out by added C_2Cl_6 powder into melt for 15 min at 690 □ in the furnace. The melt was then poured at 710 □ into a stainless steel mold with a size of 200×35×35 mm (the cooling rate was approximately 1 □/s which measured by an infrared thermometer (Raytek)). The actual chemical compositions of the experimental alloys are shown in Table 1, which measured using an X-ray Fluorescence Spectrometer (XRF, SHIMADZU XRF-1800).

Table 1.
Chemical compositions of the experimental alloys (wt.%).

Alloys	Si	Mg	Cu	Zr	Sc	Al
A	2.79	0.41	0.43	0.17	—	Bal.
B	2.84	0.39	0.45	0.19	0.57	Bal.

Specimens of the experimental alloys were taken from the central part of the casting. The samples for microstructural observations were prepared by basic metallographic preparation procedure. The polished samples were then etched using 0.5% HF solution for 25 s. The microstructural observations of the samples were performed using an MR4000 optical microscope (OM).The primary particles were identified by a HITACHI SU8020 field emission gun SEM equipped with an Oxford energy dispersive X-ray spectroscope (EDX) spectrometer. The average grain size was obtained using the linear intercept method. The crystallographic orientation were analyzed using a JSM-6490LV tungsten filament-SEM (TF-SEM) and the Channel 5 EBSD acquisition software. In order to further investigate the primary particles, a Bruker atomic force microscopy (AFM) was employed to perform three-dimensional structure analysis. Discs of 3 mm diameter for EBSD examination were prepared by mechanical ground and ion beam polishing (Gatan model 691). The samples for AFM investigation were electropolishing using a solution of 5% perchloric acid in methanol, at −30 □ with a current of 35mA.

3. Results and discussions

3.1 Microstructure observation and refining mechanism

Fig. 1 presents the typical microstructures of the two investigated casting alloys. As seen from Fig. 1(a), the thick dendrites is visible within the microstructure of unmodified alloy. The secondary dendrite arm space is close to 35 μm. With Sc addition increasing to 0.57 wt-%, the microstructure is refined significantly with fine equiaxed grain, as shown in Fig. 1(b). Moreover, a lot of particles which size are close to 6 μm are located within α-Al matrix, as marked with white arrows. A higher magnification micrograph which inserts in Fig. 1(b) shows a typical star-like primary particle. Fig. 2 shows the histogram about the average grain size of the studied alloys. As Sc addition increasing from 0 to 0.57 wt-%, the average grain size decreasing from 241.7 to 23.1 μm, which indicates that Sc is an excellent grain refiner for aluminum alloys.

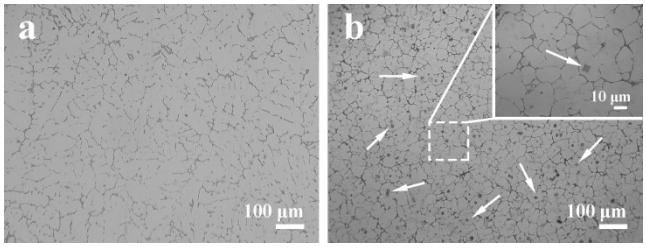

Fig. 1. OM images of (a) unmodified and (b) 0.57Sc modified alloys

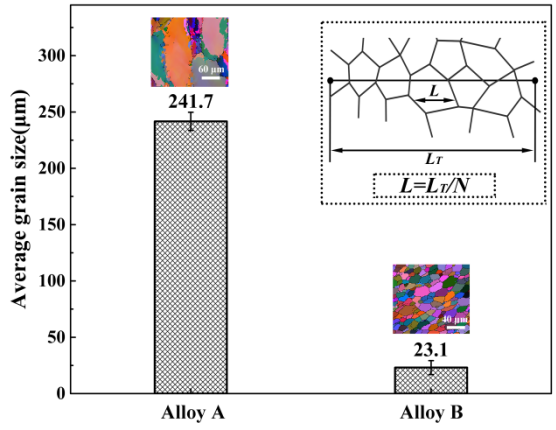

Fig. 2. Average grain size analysis of the investigated alloys

Fig. 3 shows the SEM micrographs and EDS analysis of 0.57Sc modified alloy. As shown in Fig. 3(a), a particle which size is close to 5 μm can be observed within the primary α-Al grain. The higher magnification micrograph of the selected particle exhibits an obvious multilayer structure. EDS spectrums (Fig. 3(b) and (c)) indicate that the mainly chemical compositions of the selected primary particle are Al, Sc and Zr elements. According to previous

studies [22, 23], this particle belongs to primary $Al_3(Sc, Zr)$ phase. In Fig. 3(c), the results of linear SEM-EDS show the heterogeneous distribution of Al, Sc and Zr in the primary particle, which confirms the existence of the multilayer structure of the particle. In addition, a hole which size is close to 0.4 μm can be observed at the center of the particle. The inclusion in the hole may fall off due to mechanical grinding and polishing, which serves as a nucleation site of the primary particle during solidification.

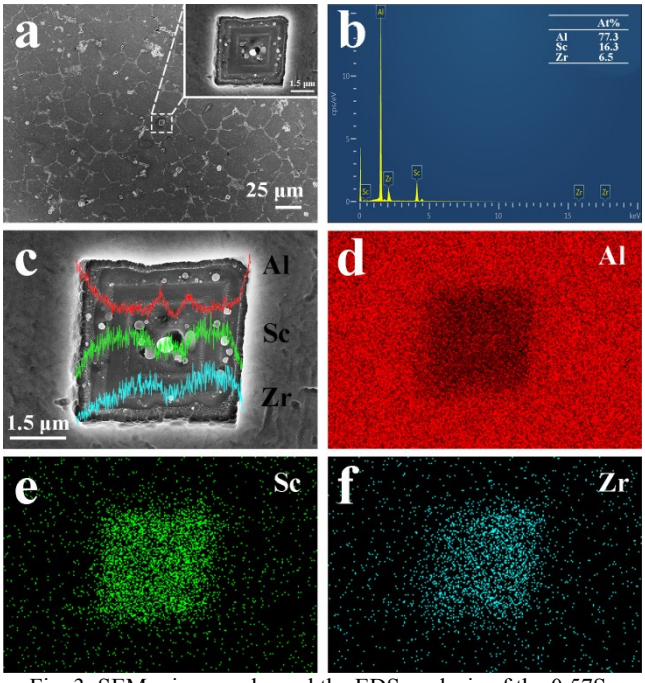

Fig. 3. SEM micrographs and the EDS analysis of the 0.57Sc modified alloy (a) typical microstructure of the 0.57Sc modified alloy; (b) EDS spectrum of a selected particle marked in Fig. 3(a); (c-f) elemental linear distribution and EDS mapping of the selected primary particle

In order to reveal the refining mechanism, EBSD measurement was conducted. Fig. 4(a) exhibits an EBSD orientation map of the 0.57Sc modified alloy, which presents the fine equiaxed grain structure with some primary particles inside. As shown in Fig. 4(b), (c), (d) and (e), square and triangular particles show similar EBSD patterns as their matrix, respectively. The interesting phenomenon confirms that the particle owns an identical orientation and similar crystal structure to the primary α-Al matrix. According to previous studies [22, 23], Al_3Sc particle owns similar $L1_2$ crystal structure to α-Al. The lattice parameter of α-Al matrix and Al_3Sc particle are 0.4050 and 0.4105 nm, respectively. Furthermore, lattice misfit between Al_3Sc particle and α-Al is further reduced by addition of Zr, which results in further grain refinement. Therefore, these particles are available as the nucleation site of α-Al matrix during solidification. A large number of nucleation core generate in liquid metal by addition of 0.57Sc, leading to a significant decreasing of average grain size.

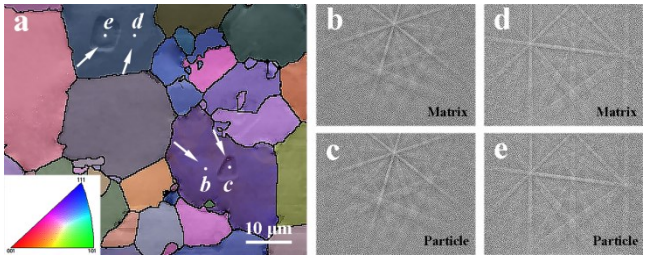

Fig. 4. (a) EBSD orientation micrograph of the 0.57Sc modified alloy; (b-e) Kikuchi patterns analysis of the 0.57Sc modified alloy, as marked with white arrows in Fig. 4(a)

3.2 Microstructural features and growth process of primary particles

Fig. 5(a), (c) and (e) present the low magnification SEM micrographs of the 0.57Sc modified alloy. As shown in Fig. 5(b), (d) and (f), several selected particles with different morphologies can be observed in the 0.57Sc modified alloy, which exhibit triangle, star, rhomboid shapes. Therefore, the particles may own cube structure. All the observed two-dimensional morphologies (Fig. 5(b), (c) and (d)) generate from sectioning the particles in different planes.

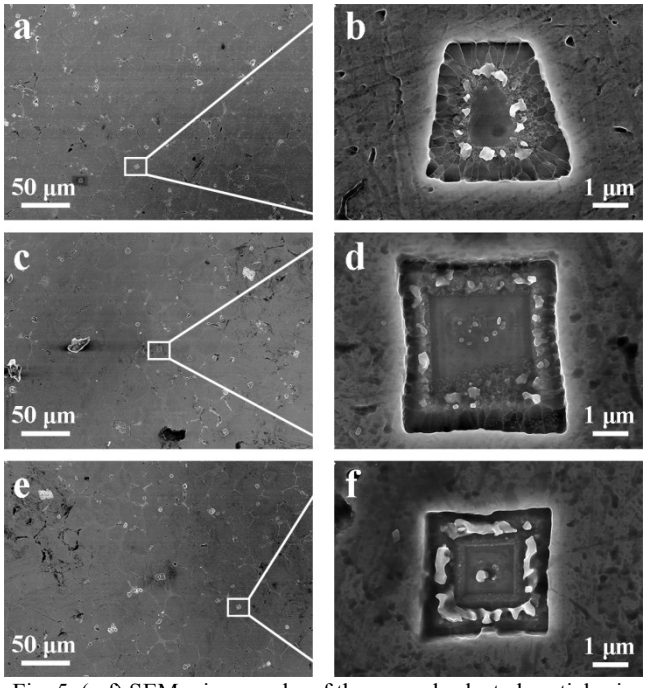

Fig. 5. (a-f) SEM micrographs of the several selected particles in different shapes observed in the 0.57Sc modified alloy

Fig. 6 shows the three-dimensional schematic diagram of the particles in different shapes observed in the 0.57Sc modified alloy. These particle with triangle, star, rhomboid shapes may generate from sectioning the particle in (111), (100) and (110) planes, respectively. Among them, the particle is sectioned in (100) plane

and shows its inner substructure clearly. In the subsequent analysis, more complex substructures could be observed within the particles which is sectioned in (100) plane.

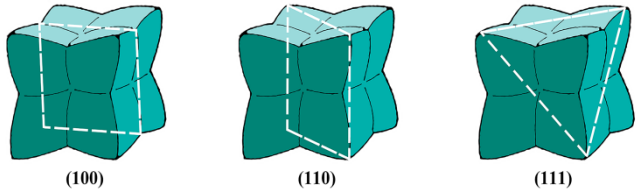

Fig. 6. Three-dimensional schematic diagram of the particles in different shapes observed in the 0.57Sc modified alloy

The typical multilayer structure morphology and corresponding elemental distribution of a selected Al_3(Sc, Zr) particle are shown in Fig. 7. In Fig. 7(a), a star-like primary Al_3(Sc, Zr) particle which sectioned in (100) plane is visible at the center of primary α-Al grain. It is found that the selected particle with a size of around 5 μm exhibits a typical five-layer structure (see Fig. 7(b)). As shown in Fig. 7(c-f), EDS analysis clearly show that the investigaed elements of particle are inhomogeneous distribution, and five different layers can be seen: the first layer with a deep hole, the second layer with Al segregation, the third layer containing concentrated Sc and Zr, the fouth layer with Al segregation and the last layer containing concentrated Sc and Zr. The central hole of the particle may generate during mechanical grinding and polishing. Therefore, the primary Al_3(Sc, Zr) particle could be eutectics which consist of two different phases. For further explore the internal structure of the primary Al_3(Sc, Zr) particles in detail, an atomic force microscopy was employed to perform three-dimensional structure analysis.

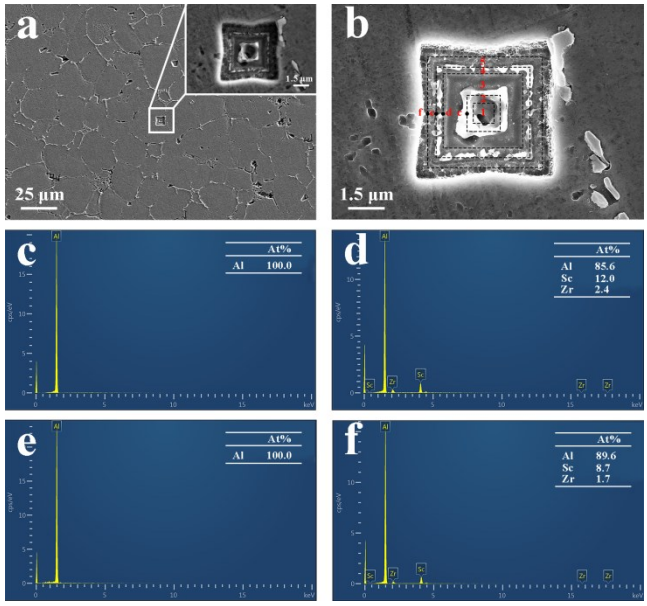

Fig. 7. (a) SEM image of the 0.57Sc modified alloy; (b) the selected primary particle showing the multilayer structure; (c-f) EDX analysis of the corresponding layer of the selected primary particle

Fig. 8 shows the three-dimensional images of three typical primary Al_3(Sc, Zr) particles which sectioned in (100) plane after electro-polishing. As shown in Fig. 8(b), (c) and (d), the primary Al_3(Sc, Zr) particles exhibit three-layer, five-layer and seven-layer structure morphology. These layers present variation in depth which indicates the different corrosion resistance of different layers during electro-polishing. The main reason is two different phases in different layers. Thus, we conclude that the primary Al_3(Sc, Zr) particles should be eutectic structure.

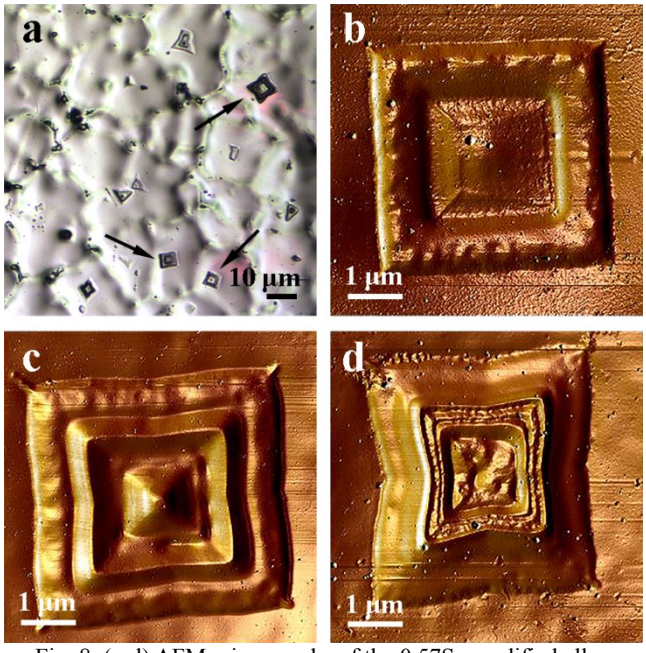

Fig. 8. (a-d) AFM micrographs of the 0.57Sc modified alloy which show different multilayer structure of the particles

Eutectic shell growth mode of the primary Al_3(Sc,Zr) particles could be seen in the 0.57Sc modified alloy. In order to illustrate the growth mechanism, a schematic diagram is shown in Fig. 9. In Fig. 9, the primary particle exhibits odd number-layer eutectic structure, which represent as (Al_3(Sc, Zr)+α-Al+ ··· +Al_3(Sc, Zr)). The growth process of the investigated particle should be discussed with the solidification sequence. Firstly, owing to the Sc content in the investigated alloy is higher than the eutectic composition, via a eutectic transformation: liquid→ Al_3Sc+α-Al, some of Sc atoms from Al_3Sc phase are replaced by Zr atoms. Thus, internal two layer of the primary particle forms. For the identical orientation and similar crystal structure between the primary Al_3(Sc, Zr) particle and α-Al matrix, the second layer of α-Al phase serve as the nucleation site for the subsequent eutectic transformation, which leads to generate odd number-layer structure at last. In addition, the cube structure morphology also exhibit concave faces and rounded corners, which caused by various gradients of constitutional supercooling in the melt.

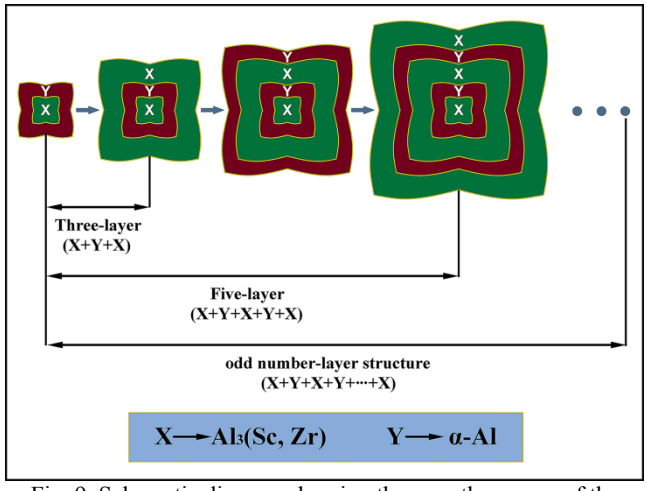

Fig. 9. Schematic diagram showing the growth process of the primary particle which observed in the 0.57Sc modified alloy

4. Conclusions

The following conclusions can be drawn from the results of the present investigation:

1. Sc is acted as an excellent grain refiner on microstructure of the studied Al-3Si-0.45Mg-0.45Cu-0.2Zr alloys. Average grain size of the investigated alloys decreases from 241.7 to 23.1 μm as Sc addition increasing from 0 to 0.57 wt-%.
2. The identical orientation and similar crystal structure between the primary α-Al phase and Al_3(Sc, Zr) particle indicates that the investigated particles serve as heterogeneous nuclei for primary α-Al phase, which significantly modify the microstructure.
3. The primary Al_3(Sc, Zr) phases own a cube structure morphology with concave faces and rounded corners, which caused by various gradients of constitutional supercooling in the melt.
4. The particle with triangle, star, rhomboid morphologies are generated from sectioning the particle in (111), (100) and (110) planes, respectively.

The primary particle exhibits typical eutectic structure containing odd number-layer, which represent as (Al_3(Sc, Zr)+α-Al+ ··· +Al_3(Sc, Zr)).

Acknowledgments

The study was financially supported by Key Technology R&D Program of Anhui Province (Grant No. 1704a0902060), Postdoctoral research foundation of Hefei University of Technology (Grant No. JZ2016HGBH1047), Science and Technology Development Program of Anhui Province (Grant No. 1501021063), Natural Science Foundation of China (Grant No. 51605128 and 51701058).

References

[1] Shu, D., Sun, B., Mi, J. & Grant, P.S. (2011). A quantitative study of solute diffusion field effects on heterogeneous nucleation and the grain size of alloys. *Acta Materialia*. 59(5), 2135-2144. DOI: 10.1016/j.actamat.2010.12.014.

[2] Men, H. & Fan, Z. (2011). Effects of solute content on grain refinement in an isothermal melt. *Acta Materialia*, 59(7). 2704-2712. DOI: 10.1016/j.actamat.2011.01.008.

[3] Górny, M., Sikora, G. & Kawalec, M. (2016). Effect of Titanium and Boron on the Stability of Grain Refinement of Al-Cu Alloy. *Archives of Foundry Engineering*. 16(3), 35-38. DOI: 10.1515/afe-2016-0045.

[4] Górny, M. & Sikora, G. (2014). Effect of Modification and Cooling Rate on Primary Grain in Al-Cu Alloy. *Archives of Foundry Engineering*. 14(3), 21-24. DOI: 10.2478/afe-2014-0054.

[5] Stjohn, D.H., Qian, M., Easton, M.A. & Cao, P. (2011). The interdependence theory: the relationship between grain formation and nucleant selection. *Acta Materialia*. 59(12), 4907-4921. DOI: 10.1016/j.actamat.2011.04.035.

[6] Mohanty, P.S. & Gruzleski, J.E. (1995). Mechanism of grain refinement in aluminium. *Acta Metallurgica et Materialia*. 43(5), 2001-2012. DOI: 10.1016/0956-7151(94)00405-7.

[7] Patakham, U., Kajornchaiyakul, J. & Limmaneevichitr, C. (2012). Grain refinement mechanism in an Al–Si–Mg alloy with scandium. *Journal of Alloys & Compounds*. 542(1), 177-186. DOI: 10.1016/j.jallcom.2012.07.018.

[8] Li, J.H., Oberdorfer, B., Wurster, S. & Schumacher, P. (2014). Impurity effects on the nucleation and growth of primary Al_3(Sc,Zr) phase in Al alloys. *Journal of Materials Science*. 49(17), 5961-5977. DOI: 10.1007/s10853-014-8315-z.

[9] Hyde, K.B., Norman, A.F. & Prangnell, P.B. (2001). The effect of cooling rate on the morphology of primary Al_3Sc intermetallic particles in Al–Sc alloys. *Acta Materialia*. 49(8), 1327-1337. DOI: 10.1016/S1359-6454(01)00050-7.

[10] Singh, V., Prasad, K.S. & Gokhale, A.A. (2004). Effect of minor Sc additions on structure, age hardening and tensile properties of aluminium alloy AA8090 plate. *Scripta Materialia*. 50(6), 903-908. DOI: 10.1016/j.scriptamat.2003.12.001.

[11] Lee, S., Utsunomiya, A., Akamatsu, H., Neishi, K., Furukawa, M., Horita, Z. & Langdon, T.G. (2002). Influence of scandium and zirconium on grain stability and superplastic ductilities in ultrafine-grained Al–Mg alloys. *Acta Materialia*. 50(3), 553-564. DOI: 10.1016/S1359-6454(01)00368-8.

[12] Cavaliere, P. & Marco, P.P.D. (2007). Friction stir processing of a Zr-modified 2014 aluminium alloy. *Materials Science & Engineering A*. 462(1-2), 206-210. DOI: 10.1016/j.msea.2006.04.159.

[13] Gao, Z.H., Li, H.Y., Lai, Y.Q., Ou, Y.X. & Li, D.W. (2013). Effects of minor Zr and Er on microstructure and mechanical properties of pure aluminum. *Materials Science & Engineering A*. 580(10), 92-98. DOI: 10.1016/j.msea.2013.05.035.

[14] Pramod, S.L., Ravikirana, Rao, A.K.P., Murty, B.S. & Bakshi, S.R. (2016). Effect of Sc addition and T6 aging treatment on the microstructure modification and mechanical properties of A356 alloy. *Materials Science & Engineering A*. 674, 438-

450. DOI: 10.1016/j.msea.2016.08.022.
[15] Xu, C., Xiao, W.L., Hanada, S.J., Yamagata, H. & Ma, C.L. (2015). The effect of scandium addition on microstructure and mechanical properties of Al–Si–Mg alloy: a multi-refinement modifier. *Materials Characterization*. 110, 160-169. DOI: 10.1016/j.matchar.2015.10.030.
[16] Emadi, D., Rao, A.K.P. & Mahfoud, M. (2010). Influence of scandium on the microstructure and mechanical properties of A319 alloy. *Materials Science & Engineering A*. 527(23), 6123-6132. DOI: 10.1016/j.msea.2010.06.042.
[17] Arfan, M., Cong, X., Wang, X.J., Shu, J.H., Hiroshi, Y., Hao, L.R. & Ma, C.L. (2014). High strength aluminum cast alloy: A Sc modification of a standard Al–Si–Mg cast alloy. *Materials Science & Engineering A*. 604, 122-126. DOI: 10.1016/j.msea.2014.03.005.
[18] Deng, Y., Yin, Z.M., Zhao, K., Duan, J.Q. & He, Z.B. (2012). Effects of Sc and Zr microalloying additions on the microstructure and mechanical properties of new Al–Zn–Mg alloys. *Journal of Alloys & Compounds*. 530(7), 71-80. DOI: 10.1016/j.jallcom.2012.03.108.
[19] Li, B., Pan, Q.L., Chen, C.P., Wu, H.H. & Yin, Z.M. (2016). Effects of solution treatment on microstructural and mechanical properties of Al–Zn–Mg alloy by microalloying with Sc and Zr. *Journal of Alloys & Compounds*. 664, 553-564. DOI: 10.1016/j.jallcom.2016.01.016.
[20] Li, B., Pan, Q.L., Huang, X. & Yin, Z.M. (2014). Microstructures and properties of Al–Zn–Mg–Mn alloy with trace amounts of Sc and Zr. *Materials Science & Engineering A*. 616, 219-228. DOI: 10.1016/j.msea.2014.08.024.
[21] Shi, Y.J., Pan, Q.L., Li, M.J., Huang, X. & Li, B. (2015). Influence of alloyed Sc and Zr, and heat treatment on microstructures and stress corrosion cracking of Al–Zn–Mg–Cu alloys. *Materials Science & Engineering A*. 621, 173-181. DOI: 10.1016/j.msea.2014.10.058.
[22] Li, J.H., Wiessner, M., Albu, M., Wurster, S., Sartory, B., Hofer, F. & Schumacher, P. (2015). Correlative characterization of primary $Al_3(Sc,Zr)$ phase in an Al–Zn–Mg based alloy. *Materials Characterization*, 102, 62-70. DOI: 10.1016/j.matchar.2015.01.018.
[23] Song, M. & He, Y.H. (2011). Investigation of primary $Al_3(Sc,Zr)$ particles in Al–Sc–Zr alloys. *Materials Science & Technology*, 26(1), 431-433. DOI: 10.1179/174328409X443236.